



Title	Adrenal Imaging with $^{131}\text{I}$ -Adosterol (NCL-6- $^{131}\text{I}$ ) by Diverging and Pinhole Methods I I.Analysis of Normal Adrenal Images
Author(s)	中條, 政敬
Citation	日本医学放射線学会雑誌. 1981, 41(10), p. 985-997
Version Type	VoR
URL	<a href="https://hdl.handle.net/11094/16318">https://hdl.handle.net/11094/16318</a>
rights	
Note	

*The University of Osaka Institutional Knowledge Archive : OUKA*

<https://ir.library.osaka-u.ac.jp/>

The University of Osaka

# Adrenal Imaging with $^{131}\text{I}$ -Adosterol (NCL-6- $^{131}\text{I}$ ) by Diverging and Pinhole Methods

## I. Analysis of Normal Adrenal Images

Masayuki Nakajo

Department of Radiology, Kagoshima University School of Medicine, Kagoshima 890, Japan

(Director: Prof. S. Shinohara)

Research Code No.: 730

Key Words: Adrenal imaging,  $^{131}\text{I}$ -Adosterol, Normal adrenal gland, Diverging collimator, Pinhole collimator

## ディバージング及びピンホール法による $^{131}\text{I}$ -Adosterol (NCL-6- $^{131}\text{I}$ ) 副腎シンチグラフィ

### I. 正常副腎像の解析

鹿児島大学医学部放射線医学教室 (主任: 篠原慎治教授)

中 條 政 敬

(昭和56年2月3日受付)

(昭和56年4月21日最終原稿受付)

$^{131}\text{I}$ -Adosterol による正常副腎80例の diverging 及び pinhole 像が解析された. diverging 像による両副腎の位置的高低に関しては, 右高55例 (69%), 同高24例 (30%), 左高1例 (1%) であった. 両副腎の activity に関しては, 後面像と前面像では相違がみられ, 後面像での右高50例 (62.5%), 同高26例 (32.5%), 左高4例 (5%) に対し, 前面像では各々, 13例 (16%), 55例 (69%), 12例 (15%) であった. コンピュータ処理可能72例について, 各副腎領域の counts を算出し, 左右比・後面前面比を求めた. 左右比では後面像の右高比が前面像で減少ないし左高比に逆転したものの47例, 左高比が前面像で増大したものの5例が認められ, また後面前面比は右が左よりも52例 (72%) で大であった. この両体位における activity

の相違は, 側面像及び副腎の周囲臓器との関係より, 両副腎の深さ, 周囲臓器による  $^{131}\text{I}$  の減弱及び肝による activity の overlap の相違の三因子で説明可能であった. 各体位での net counts の左右比も求めたが, それは両副腎の深さの相違より生ずる counts 差は補正されていないので, 真の左右比とは言い難く, 両体位での各副腎の net counts の和の比を求め, 真の比の近似値とした. これによると右高比は51例 (71%, 平均: 1.37, 範囲: 1.01—3.15), 左高比は21例 (29%, 平均: 1.14, 範囲: 1.01—1.41) であった. 右高群に偏位例が多く認められたが, これは左副腎の描出不良に起因した. pinhole 像により左右副腎の形態的分類を試みた. 左副腎は楕円形 (64%) > 三角形 (25%) > 円形 (11%) であったのに対し, 右

副腎は三角形(64%)>楕円形(25%)>円形、鎌状形(11%)であった。左右副腎内の打点分布には各々特徴があり、左は頭内側ないし内側で activity が高いものが74%を、一方右では中央部

が高く末梢に向い緩かに減少するものが76%を占めた。これらの正常副腎像の解析より、副腎シンチグラムの読影上の注意点について論じた。

### Introduction

Following the first synthesis of  $^{125}\text{I}$ -19-iodocholesterol in 1969<sup>1)</sup>, visualization of the adrenal glands could be achieved in dogs with it<sup>2)</sup> and in humans with  $^{131}\text{I}$ -19-iodocholesterol<sup>3)</sup>. Consequently the latter agent had received considerable publicity in clinical use as an adrenal imaging agent. In 1975, however, a new adrenal imaging agent,  $^{131}\text{I}$ -Adosterol (NCL-6- $^{131}\text{I}$ , 6 $\beta$ -iodo-methyl-19-norcholest-5(10)-en-3 $\beta$ -ol- $^{131}\text{I}$ )<sup>4)</sup> or  $^{131}\text{I}$ -NP-59<sup>5)</sup> was reported and it has been revealed to be a superior agent compared with  $^{131}\text{I}$ -19-iodocholesterol.

Although the clinical diagnostic value of these two agents in the assessment of patients suspected of having Cushing's syndrome<sup>6)</sup>, aldosteronism<sup>7,8)</sup> and pheochromocytoma<sup>9)</sup> was documented, only a few reports have been published concerning analysis of normal adrenal images<sup>10,11)</sup> and detailed analysis has not been fully made in terms of their morphological aspects. In my department,  $^{131}\text{I}$ -19-iodocholesterol was used for a period of approximately one year from 1973. From 1975 to the present,  $^{131}\text{I}$ -Adosterol has been used. Our initial study on adrenal scintigraphy with  $^{131}\text{I}$ -19-iodocholesterol using a diverging collimator revealed the interrelationship of bilateral normal adrenal radioactivities<sup>10)</sup>. The diagnostic difficulty with diverging images, however, was encountered frequently because of their morphological inferiority. The subsequent effort to obtain more improved adrenal images led us to the use of a pinhole collimator for adrenal scintigraphy<sup>12)</sup>.

In this paper, the analysis of normal adrenal diverging and pinhole images with  $^{131}\text{I}$ -Adosterol is made in order to establish the normal adrenal imaging patterns which will be fundamental for the correct interpretations of various adrenal images.

### Materials and Methods

Since February 1975, more than 200 adrenal imagings have been performed on patients with known or suspected adrenal diseases and on normal volunteers. Of these imagings, 80 have been done on 5 normal volunteers and 75 patients in whom the subsequent studies (urinary and plasma chemistries, venography, arteriography and/or CT) revealed no evidence of adrenal diseases. Their adrenal images were reviewed and analyzed. All individuals received about  $16\mu\text{Ci/kg}$  of body weight of  $^{131}\text{I}$ -Adosterol intravenously which was provided to us by Daiichi Radioisotopes Laboratory LTD., Japan.

The adrenal imaging was performed 5-9 days postinjection to determine the location of each gland by using a diverging collimator. Each adrenal image was then separately obtained on Polaroid film with the use of a pinhole collimator, closely applied to the marked point on the patient's back in prone position (Pinhole method). Posterior and anterior diverging images were obtained to evaluate the anatomical and radioactive relationships between both glands, 12-14 days after injection when the hepatic radioactivity had almost disappeared (Diverging method). Lateral diverging and/or pinhole images were also obtained in selected subjects in prone position mainly to determine the adrenal depth. All these images were obtained with preset counts of 22 k, using a gammacamera (RC-1C-1205, HITACHI, Japan) coupled with a minicomputer (HITAC 10).

To block the thyroidal accumulation of  $^{131}\text{I}$ , each patient was administered KI powder 0.3 g a day orally, beginning one day before the tracer injection and continuing 6 days postinjection. Laxatives were administered to eliminate bowel radioactivity in most subjects.

Presented, in part, at the 19th Annual Meeting of the Japanese Society of Nuclear Medicine, Tokyo, Nov. 26-29, 1979.

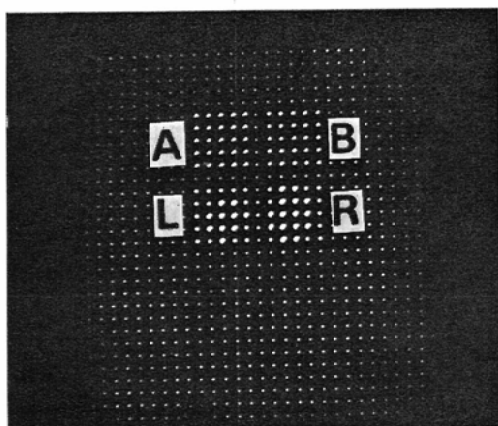


Fig. 1 The method of ROI setting on the smoothing diverging image (posterior view).

The upper ROIs show the left (A) and right (B) background regions and the lower ones, the left (L) and right (R) adrenal regions.

The original diverging images were used to analyze the anatomical and radioactive relationships between both glands. Also, a semiquantitative analysis was made in 72 subjects by obtaining various count ratios using a minicomputer as follows: The same sized ROIs of each adrenal region and the background one above it were set to calculate their counts on the posterior and anterior diverging smoothing displays (Fig. 1).

1. Adrenal region high/low ratio = High A.R.C.\*/Low A.R.C.
2. Adrenal P/A ratio = R (L)-posterior A.R.C./R (L)-anterior A.R.C.
3. Adrenal high/low ratios
  - 1) Adrenal high/low ratio on each view = Posterior (anterior) high net counts (A.R.C. — B.R.C.\*\*)/Posterior (anterior) low net counts (A.R.C. — B.R.C.)
  - 2) Adrenal high/low ratio on both views = High (anterior + posterior) net counts/Low (anterior + posterior) net counts

\*Adrenal region counts, \*\*Background region counts.

The original pinhole images were used to analyze the adrenal morphological aspects. Classification of the adrenal types were made on each adrenal side, depending upon the outline and inner radioactive distribution. The longitudinal/transverse ratio was obtained by measuring the longest longitudinal and transverse diameters of the adrenal on the pinhole image.

The computer processed displays such as 2 and/or 3 dimensional ones after smoothing was performed in selected subjects.

The renal imaging with  $^{99m}\text{Tc}$ -DMSA and combined renal and adrenal imaging were also performed to clarify the scintigraphic relationship between them in some subjects.

## Results

### I. Analysis of normal adrenal diverging images

#### 1) Positional relationship

On the original posterior view, the right adrenal gland was located slightly higher than the left in 55 of the 80 subjects (69%). In the majority of them, the right gland was located 1-3 cm higher than the left. In 24

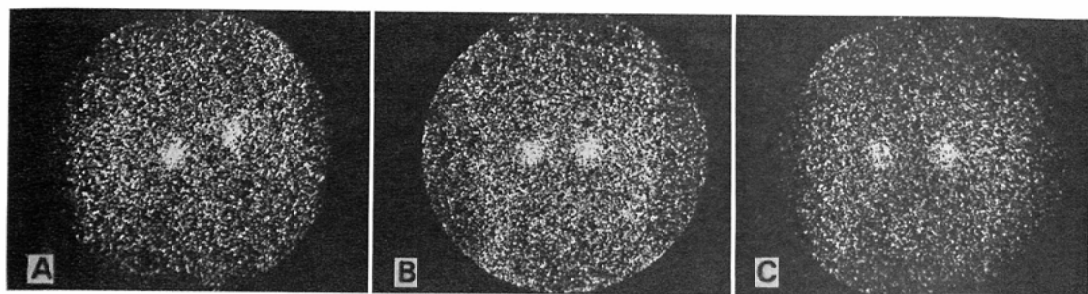


Fig. 2 Positional relationship between both glands.

A: right higher image, B: same level image, C: left higher image.

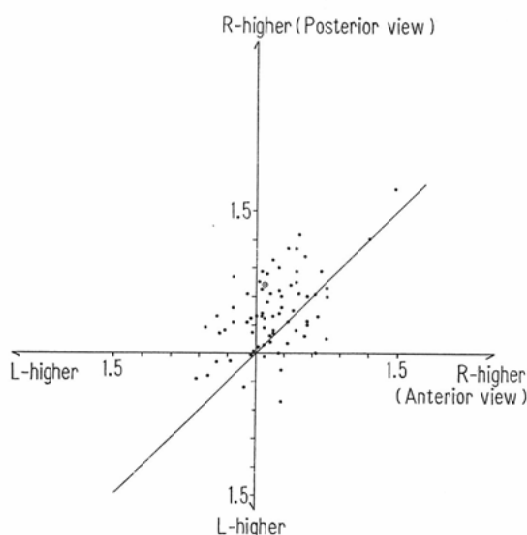


Fig. 3 The relationship of the adrenal region high/low ratios between both views.

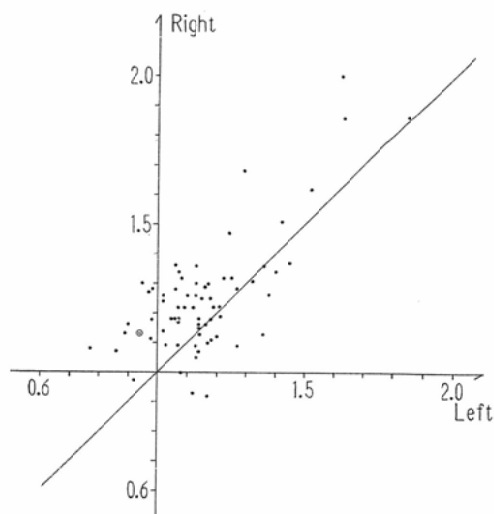


Fig. 4 The relationship of the adrenal P/A ratios between both glands.

(30%), the superior borders of the two glands were at the same level and in only 1, the left gland seemed to be slightly higher than the right (Fig. 2).

## 2) Radioactivity over the adrenal region

On the original posterior view, the radioactivity of the right gland appeared greater than that of the left in 50 of the 80 subjects (62.5%). In 26 (32.5%), both glands showed nearly the same radioactivity and that of the left appeared to be greater in only 4 (5%). On the anterior view, both glands showed nearly the same radioactivity in 55 subjects (69%), that of the right gland appeared to be higher than that of the left in 13 and lower in 12. The relationship of the adrenal region high/low ratios between posterior and anterior views is shown in Fig. 3. The right higher ratio was observed in 60 of the 72 subjects (83%) on the posterior view, whereas a higher ratio was shown in 53 of the subjects (74%), on the anterior view. The posterior right higher ratio was larger than the anterior one in 35 subjects and was inverted to the left higher ratio on the anterior view in 12. The posterior left higher ratio was smaller than the anterior one in 5 of the subjects. The relationship of the adrenal P/A ratios between both glands is shown in Fig. 4. The P/A ratio of the right gland was higher than that of the left in 52 subjects (72%). These results indicate that in most normal subjects, the decreasing degree of the ad-

renal radioactivity from the posterior view to the anterior view is greater in the right gland than in the left. This adrenal radioactive discrepancy between posterior and anterior views can be explained by three possible factors. The first factor is the difference in depth between the right and left adrenals; the left lateral view in most normal subjects revealed two hot areas which were partially overlapped (Fig. 5). The posterocephaled hot spot indicates the right adrenal radioactivity and the anteroceudad one, the left. On the anterior view, the relationship of the distance between each gland and the detector surface is reversed to that on the posterior view. The second factor is the difference of  $^{131}\text{I}$  attenuation from each gland due to its surrounding organs; the right gland has no organs behind it, however, the liver, a large parenchymatous organ, exists anteriorly. On the left side, the left kidney is behind the left gland and the pancreas, a relatively small organ, is located in front of it. These anatomical relationships have been visualized by CT (Fig. 6). On the posterior view, the photon attenuation of  $^{131}\text{I}$  from the left gland is greater than the right, and on the anterior view, the reverse. The third factor is the overlapping radioactivity from the liver to the right adrenal. The results mentioned above suggest that both adrenal radioactivities on the posterior and anterior image are apparent. Consequently, the author tried to obtain the true adrenal high/low ratio. Fig. 7 shows the relationship of the adrenal high/low ratios between both views. On the posterior view, the right higher ratio was observed in 60 subjects (mean; 1.46, range; 1.01-3.47) and the left higher ratio in 12 (mean; 1.24, range; 1.04-1.64). On the anterior view, the right higher ratio was observed in 42 subjects (mean; 1.37, range; 1.01-2.73) and the left higher ratio in 30 (mean; 1.29, range; 1.01-2.54). The tendency that the posterior right higher ratio was larger than the anterior ratio or inverted to

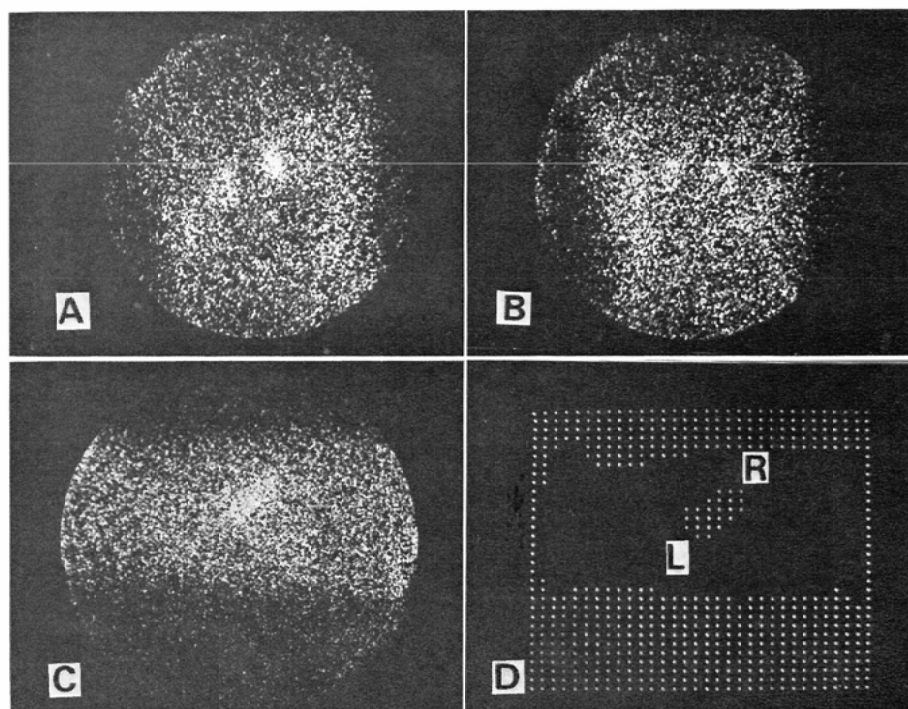


Fig. 5 Typical normal adrenal diverging images.

The right adrenal radioactivity is higher than the left one on the posterior view (A), however both are almost equal on the anterior view (B). The left lateral original (C) and computer-processed (D) views show the right gland located more posteriorly than the left.

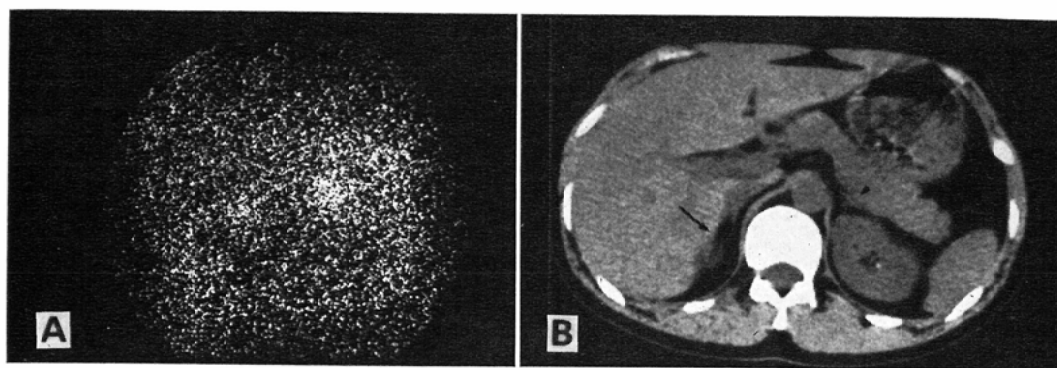


Fig. 6 Comparison of the posterior adrenal image with the CT.

The right adrenal radioactivity is considerably higher than the left one on the posterior view (A). The same patient's CT at the adrenal level (B) reveals the right gland (arrow) located more posteriorly than the left (arrow head). In addition, the transverse relationship between each gland and its surrounding organs are clearly demonstrated (see text).

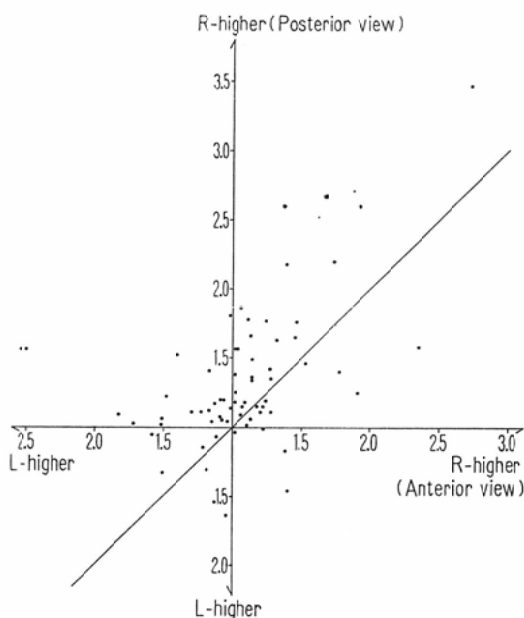


Fig. 7 The relationship of the adrenal high/low ratios between both views.

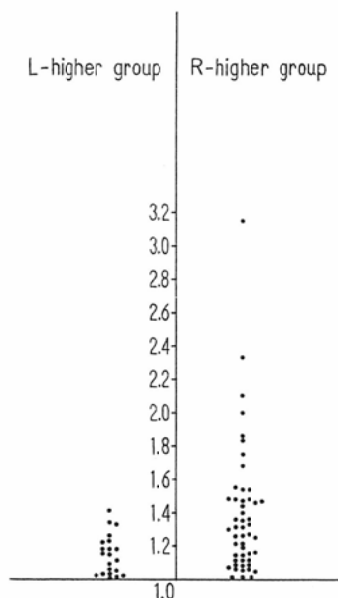


Fig. 8 Adrenal high/low ratios on both views.

the left higher ratio on the anterior view and the posterior left higher ratio was smaller than the anterior ratio was also found in most subjects as was observed in the adrenal region high/low ratios. Although this high/low ratio on each view is free from the influence of the background radioactivity theoretically, the difference of the adrenal counts produced by that of the adrenal depth cannot be corrected. To correct it, the sum of each adrenal posterior and anterior net counts were obtained. The result of these adrenal high/low ratios on both views is shown in Fig. 8. The right higher ratio was observed in 51 subjects (71%) and the left higher ratio in 21 (29%). The right higher ratio ranged from 1.01 to 3.15, with a mean ratio of 1.37 and the left ratio ranged

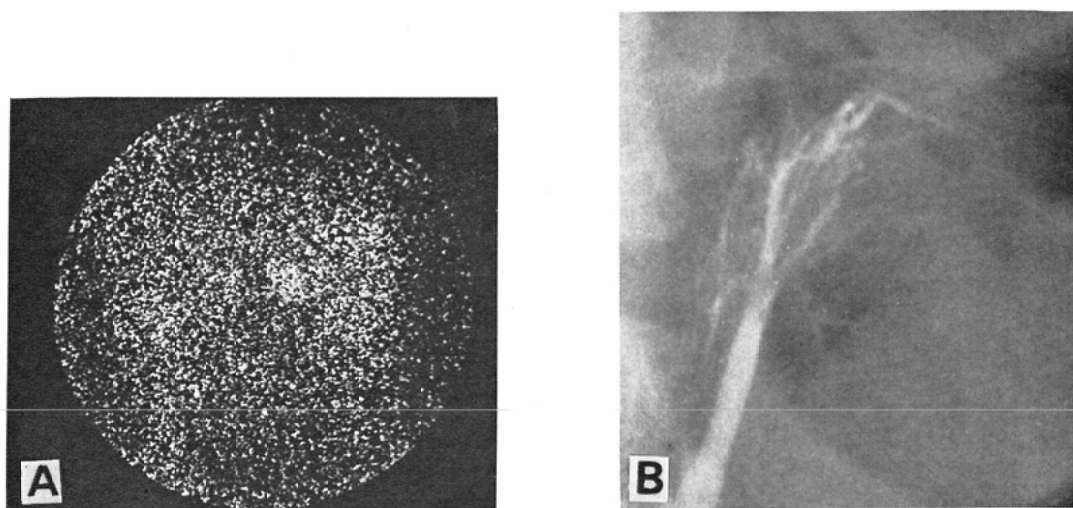


Fig. 9 Remarkably asymmetrical normal image and its venographic finding.

The faint visualization of the left gland resulted in remarkably asymmetrical uptake on the posterior view (A). The adrenal venography revealed normal appearance of the left gland (B).

from 1.01 to 1.41, with a mean ratio of 1.14. The high deviation values were obtained in the right higher group. Those were due to the low radioactivities of the left glands. The remarkably asymmetrical posterior diverging image is shown in Fig. 9.

## II. Analysis of normal adrenal pinhole images

### 1) Morphological classification

Although various types were observed in the normal adrenal images, they were basically divided into oval, triangular, round and sickle. Fig. 10 shows the left adrenal imaging types. The oval types were subdivided into the cephalo-pointed (A), cephalo-rounded (B) and pure (C). The former two showed relatively high radioactivity in the upper medial portion of the gland and that of the latter was high in its midportion. The triangular types were subdivided into two; the regular one (D) whose radioactivity was high in the upper portion and the crescent one (E) whose medial portion showed higher radioactivity. The last type was the round one (F). Fig. 11 shows the right adrenal types. The triangular types were subdivided into the regular (A) and isosceles (B) one. The two oval types (C, D) differed in the direction of their longer axes. The other types showed round (E) and sickle (F) appearances.

### 2) Frequency and other data

Fig. 12 shows various data concerning the normal adrenal types. On the left side, the oval types were the most predominant (64%) followed by the triangular ones (25%). On the right side, the triangular types were the most predominant (64%) followed by the oval ones (25%). The longitudinal/transverse ratios of the various adrenal types were all more than 1.0 except that of one right triangular type which was 0.9. Characteristic radioactive distributions were observed in both glands respectively. 74% of the left glands showed higher radioactivity in their upper and/or medial portions. In 76% of the right glands, the activity was higher in its midportion and decreased gradually toward the peripheral site. The 90°-rotated 3-dimensional display demonstrated clearly the appearance of the radioactive distribution in each image (Fig. 10 and 11).

The left lateral pinhole image revealed the posteroanterior relationship between both glands not only more clearly than the diverging image, but also the condition that each gland lay obliquely from the posterocephalad



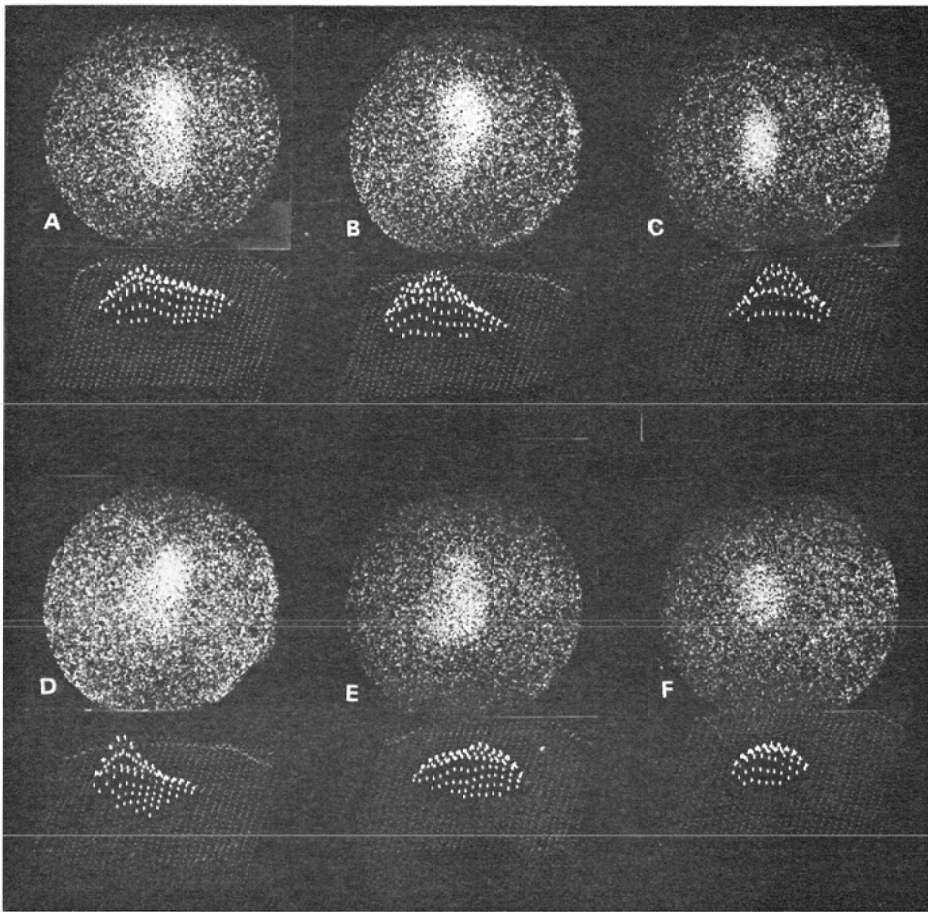


Fig. 10 Types of left normal adrenal glands. See text.

A, B, C: oval types, D, E: triangular types, F: round type. The 90°-rotated 3-dimensional display is shown below each original posterior view.

to the anterocaudal direction (Fig. 13).

The combined posterior images of each adrenal gland and kidney demonstrated the anatomical relationship between them. Most of the left gland overlapped the medial upper portion of the left kidney, whereas that of the right one was above the upper pole of the right kidney (Fig. 14).

#### Discussion

The results obtained by the analysis of normal adrenal diverging images with  $^{131}\text{I}$ -Adosterol in this study are similar to our previous report obtained with  $^{131}\text{I}$ -19-iodocholesterol<sup>10)</sup> and the results reported by Freitas et al. with  $^{131}\text{I}$ -NP-59<sup>11)</sup>.

Recognition of the location of both adrenal glands, the right being slightly higher than the left or both at the same level in a majority of normal subjects may be useful for detection of the abnormality of the adrenal location due to the adrenal lesion itself or the effect of pressure caused by the extra-adrenal lesions.

High radioactivity of the right gland compared with the left on the routinely used posterior view and its re-

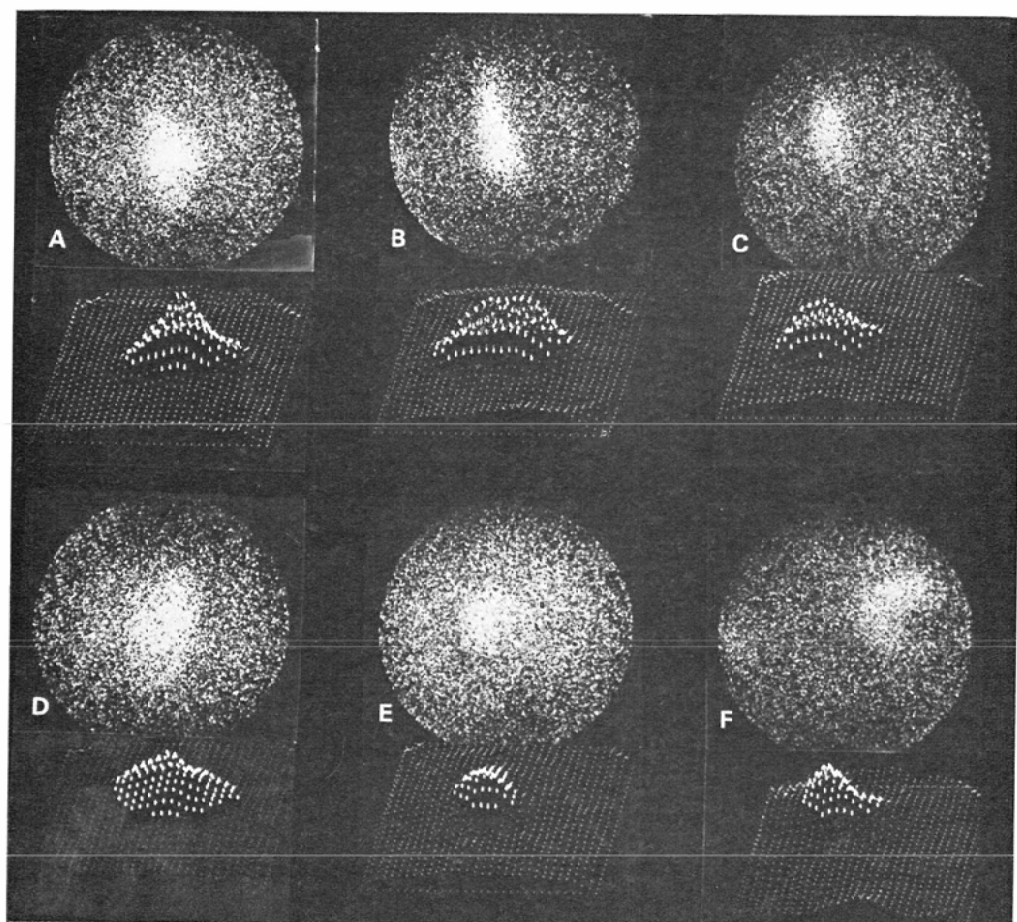


Fig. 11 Types of right normal adrenal glands. See text.

A, B: triangular types, C, D: oval types, E: round type, F: sickle type.

versal tendency on the anterior view in most normal subjects can be explained by differences in adrenal depth, attenuation of  $^{131}\text{I}$  from each adrenal due to its surrounding organs and overlapping radioactivity from the liver. Recent use of computed tomography has made it easy to clarify the transverse anatomical relationship between each gland and its surrounding organs. The CT findings of normal adrenal glands are also useful for the explanation of the normal diverging images<sup>13)</sup>.







The marked variation in the normal adrenal posterior diverging image in this series was due to the faint image of the left gland. Faint visualization of the left gland with the normal radioactivity of the right does not always represent left adrenal abnormality itself. Conversely, if the right gland uptake is considerably lower than the left on the posterior view, the abnormality of either gland is considered a definite possibility.

The result of adrenal high/low ratios on both views in the normal subjects suggest that the left higher ratio may have the diagnostic value but the right higher one may be less indicative because of the large deviation in the ratio.

Although the comparison of the radioactivity between both glands is one of the important diagnostic points, there is the possibility of making a misinterpretation, unless the normal asymmetry mentioned above is

A. Left adrenal glands

B. Right adrenal glands

Type	Schema	Longitudinal Transverse ratio		No. of adrenals		Frequency (%)
		Mean	Range			
Oval		1.9	1.2~2.6	23	51	64
		2.0	1.5~2.3	19		
		2.1	1.7~2.5	9		
Triangular		1.3	1.1~1.7	18	20	25
		1.4	1.3~1.5	2		
Round		1.1	1.0~1.3	9	9	11







Type	Schema	Longitudinal Transverse ratio		No. of adrenals		Frequency (%)
		Mean	Range			
Triangular		1.4	0.9~2.3	29	51	64
		2.0	1.4~2.7	22		
Oval		1.8	1.4~3.2	12	20	25
				8		
Round or Sickle		1.2	1.0~1.3	6	9	11
		1.7	1.7~1.8	3		

Fig. 12 Results of normal adrenal pinhole images.

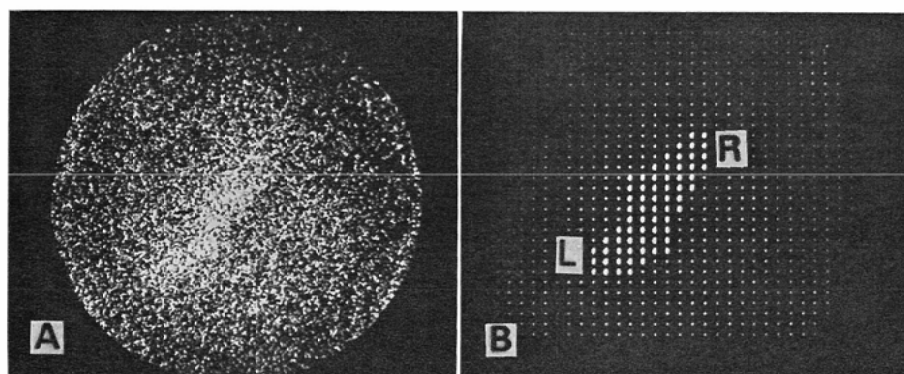


Fig. 13 Left lateral normal pinhole images. See text.

A: the original image, B: the computer-processed display.

recognized. Furthermore, no radioactive lateralization was seen in some patients with aldosteronomas and adversely, some patients with idiopathic aldosteronism showed asymmetrical uptakes by both glands<sup>7)</sup>. The limitation of the diagnosis which mainly depends upon the radioactive comparison between both glands will be discussed in detail in Part II.

As the pinhole image has high-resolution, the scintigraphic diagnosis of the adrenal abnormality can be made depending upon the morphological appearance of each gland rather than the radioactive comparison between both glands. It is very important to establish the normal pinhole imaging pattern for the correct interpretation. Although the normal adrenal pinhole images were classified tentatively, even the same nominal basic type differed between both glands. The decreased radioactivity in the lower lateral portion of the left gland in most normal subjects may represent the concave impression produced by the convex surface of the left kidney.

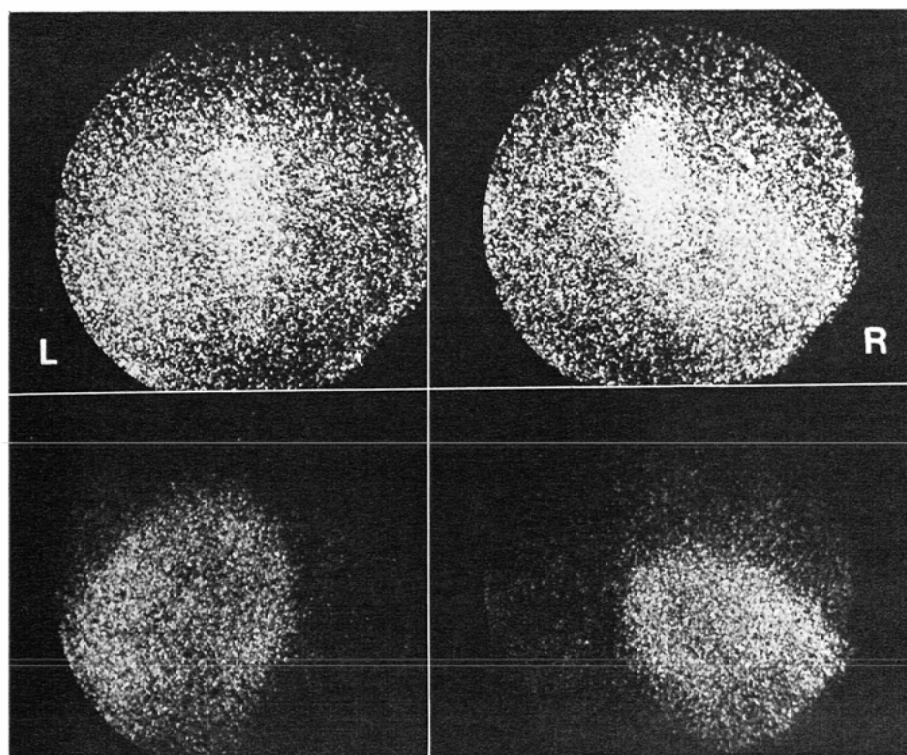


Fig. 14 Scintigraphic relationship between the adrenal gland and the kidney. See text.

The upper images represent the combined images of each adrenal gland and kidney. The outline of each kidney at the same imaging position as taken from each combined image is shown below it.

The loose attachment of the right adrenal to the kidney accounts for a homogeneous radioactive distribution which shows a peak at the midportion of the gland<sup>14)</sup>.

Consideration of the shape and the radioactive distribution of each normal adrenal gland is very important. If one fails to recognize the characteristics of the normal adrenal images, the high radioactivity in the upper portion of the left may be misinterpreted as an adenoma or the concave decreased radioactive area in its lower lateral portion and the concave curve of the sickle type of the right, as a space occupying "cold" lesion such as a pheochromocytoma. Conversely, if a hot or cold area is noted in the portion beside the normally recognized sites, the possibility of its abnormality is thought to be high. As the longitudinal/transverse ratio of the adrenal gland was more than 1.0 in almost all normal glands, the ratio below 1.0 could also indicate the adrenal abnormality.

In my initial experience of the diverging imaging with  $^{131}\text{I}$ -Adosterol in normal subjects, the left gland was visualized faintly 3 days postinjection. The right, however, could not be detected because of the hepatic overlapping radioactivity. Both glands were visualized from 5 or 6 to 14 days (the end of the follow-up imaging) postinjection. Therefore the Pinhole method was performed 5–9 days according to the patient's circumstances. If the early imaging could not provide good quality images, the reimaging was performed 2 days after it. In most normal subjects, each gland was visualized most clearly in the 7–9th day. Although the imaging time of each gland differed depending upon the period after the injection, the administered dose of the tracer, the depth from the tip of a pinhole collimator to the adrenal and its uptake dose, it was in the range of 10 to 20

minutes and the left gland usually required a slightly longer imaging time than the right. Both adrenal imaging times ranged approximately from 20 to 40 minutes. Although it is a long time, this is not an essential problem because the purpose of the examination is to obtain the detailed information necessary to make the correct diagnosis.

Despite the fact that a pinhole collimator has been used routinely for thyroid imaging and its superiority was documented<sup>15)16)</sup>, this collimator has not been widely used for adrenal imaging. There are two reasons for this: The first one is the prolonged imaging time due to the low adrenal uptake (mean; 0.16%, range; 0.07–0.26%/normal gland by an external counting method<sup>11)</sup>) compared with the uptake of iodine by the thyroid. The second one is the difficulty in collimating the adrenals. If a more superior adrenal imaging agent appears in the future, the disadvantage of the Pinhole method will be overcome.

### Conclusion

The adrenal diverging and pinhole images with <sup>131</sup>I-Adosterol in 80 subjects with no evidence of adrenal diseases were analyzed to establish the normal adrenal imaging patterns.

The results obtained from the analysis of the diverging images were as follows:

- 1) The right gland was located higher than the left in 69% of the subjects and in 30% both adrenals were located at the same height. In only one subject, the left adrenal was slightly higher than the right.
- 2) On the posterior view, the right higher asymmetrical uptake was observed in most subjects (62.5%), whereas the symmetrical uptake was most frequently (69%) seen on the anterior view. This discrepancy could be explained by differences in depth, photon attenuation and hepatic overlapping radioactivity between both glands.
- 3) The adrenal high/low ratio on both views, semiquantitative comparison between both adrenal radioactivities, showed a higher deviation in the right higher group (mean; 1.37, range; 1.01–3.15) than in the left higher one, however, its deviation was small (mean; 1.14, range; 1.01–1.41). The high deviation values were due to the low uptake of the left glands.

The results obtained from the analysis of the pinhole images were as follows:

- 1) Although the scintigraphic morphology differed essentially between both glands, the left glands were basically divided into oval (64%), triangular (25%), and round (11%) types, whereas the right glands were divided into triangular (64%), oval (25%) and round or sickle (11%) types.
- 2) The inner radioactive distributions of both glands were characteristic respectively. In 74% of the subjects, the left gland showed higher radioactivity in its upper and/or medial portion, and the radioactivity of the right was higher in its midportion and decreased toward its peripheral region in 76%.

According to these results, the important points on interpretation of the adrenal images were discussed.

### Acknowledgment

This research was conducted under the direction of Professor Shinji Shinohara. Grateful acknowledgment is made to him for his constant interest and valuable criticism. Thanks are also tendered to the staff of the Department of Radiology for their collaboration.

### References

- 1) Counsell, R.E., Ranade, V.V., Blair, R.J., Beierwastes, W.H. and Weinhold, P.A.: Tumor localizing agents. IX. Radioiodinated cholesterol. Steroid, 16: 317–328, 1970
- 2) Blair, R.J., Beierwaltes, W.H., Lieberman, L.M., Boyd, C.M., Counsell, R.E., Weinhold, P.A. and Varma, V.M.: Radiolabeled cholesterol as an adrenal scanning agent. J. Nucl. Med., 12: 176–182, 1971

- 3) Beierwaltes, W.H., Lieberman, L.M., Ansari, A.N. and Nishiyama, H.: Visualization of human adrenal gland in vivo by scintillation scanning. *JAMA*, 216: 275—277, 1971
- 4) Kojima, M., Maeda, M., Ogawa, H., Nitta, K. and Ito, T.: New adrenal scanning agent. *J. Nucl. Med.*, 16: 666—668, 1975
- 5) Sarkar, S.D., Beierwaltes, W.H., Basmadjian, G.P., Hetzel, K.R., Kennedy, W.P. and Manson, M.M.: A new and superior adrenal scanning agent, NP-59. *J. Nucl. Med.*, 16: 1038—1042, 1975
- 6) Moses, C.M., Schteingart, D.E., Sturman, M. F., Beierwaltes, W.H. and Ice, R.D.: Efficacy of radiocholesterol imaging of the adrenal glands in Cushing's syndrome. *Surg. Gynecol. Obstet.*, 139: 201—204, 1974
- 7) Seabold, J.E., Cohen, E.L., Beierwaltes, W.H., Hinerman, D.L., Nishiyama, R.H., Bookstein, J.J., Ice, R.D. and Balachandran, S.: Adrenal imaging with  $^{131}\text{I}$ -19-iodocholesterol in the diagnostic evaluation of patients with aldosteronism. *J. Clin. Endocrinol. Metab.*, 42: 41—51, 1976
- 8) Freitas, J.E., Grekin, R.J., Thrall, J.H., Gross, M.D., Swanson, D.P. and Beierwaltes, W.H.: Adrenal imaging with iodomethyl-norcholesterol (I-131) in primary aldosteronism. *J. Nucl. Med.*, 20: 7—10, 1979
- 9) Sturman, M.F., Moses, D.C., Beierwaltes, W.H., Harrison, J.S., Ice, R.D. and Dorr, R.P.: Radiocholesterol adrenal images for the localization of pheochromocytoma. *Surg. Gynecol. Obstet.*, 138: 177—180, 1974
- 10) Nakajo, M., Higuchi, K., Sonoda, K. and Shinohara, S.: Clinical study of adrenal scintigraphy with  $^{131}\text{I}$ -19-cholesterol —with reference to analysis of normal adrenal scintigram—. *Jap J. Clin. Radiol.*, 22: 97—102, 1977
- 11) Freitas, J.E., Thrall, J. H., Swanson, D.P., Rifai, A. and Beierwaltes, W.H.: Normal adrenal asymmetry: explanation and interpretation. *J. Nucl. Med.*, 19: 149—153, 1978
- 12) Nakajo, M., Higuchi, K., Sakata, H., Shinohara, H. and Sonoda, K.: Adrenal scintigraphy using a pinhole collimator. *Nipp. Act. Radiol.*, 38: 340—353, 1978
- 13) Montagne, J.P., Krassel, H.Y., Korobkin, M. and Moss, A.A.: Computed tomography of the normal adrenal glands. *Am. J. Roentgenol.*, 130: 963—966, 1978
- 14) Kahn, P.C.: Adrenal arteriography. In angiography, and edition, Abrams, H.L., ed. Boston, Little, Brown & Co, 929—940, 1971
- 15) Hurley, P.J., Straus, H.W., Pavoni, P., Langan, J.K. and Wagner, H.N.: The scintillation camera with pinhole collimator in thyroid imaging. *Radiology*, 101: 133—138, 1971
- 16) Sostre, S., Anshare, A.B., Quinones, J.D., Schieve, J.B. and Zimmerman, J.M.: Thyroid scintigraphy: pinhole images versus rectilinear scans. *Radiology*, 129: 759—762, 1978